

# Fabrication of Detonation Nanodiamonds Containing Silicon-Vacancy Color Centers by High Temperature Annealing

Konosuke Shimazaki, Hiroki Kawaguchi, Hideaki Takashima, Takuya Fabian Segawa,\*  
Frederick T.-K. So, Daiki Terada, Shinobu Onoda, Takeshi Ohshima,  
Masahiro Shirakawa, and Shigeki Takeuchi\*

Detonation nanodiamonds (DNDs) with sizes below 10 nm have attracted attention as single photon emitters with potential in many research fields from life sciences to quantum technologies. However, while nitrogen-vacancy (NV) color centers are found in nanodiamonds directly after the detonation synthesis without the need for irradiation or annealing, silicon-vacancy (SiV) color centers are not present in these pristine samples. Herein, SiV centers are created in DNDs by an annealing treatment up to 1100 °C in high vacuum. As silicon is not added, the precursor of the SiV centers must be pristine silicon impurities inside the nanodiamond lattice. A sharp emission line at the wavelength of 737 nm with a linewidth of 7.7 nm is observed in DNDs that are electron irradiated before annealing. This wavelength is consistent with the characteristic emission line of SiV centers and its linewidth is comparable with that in larger nanodiamonds created by chemical vapor deposition and subsequent milling. The average lifetime ( $0.4 \pm 0.04$  ns) of the fluorescence, which is in the range of reported lifetimes in nanodiamonds, also support that the observed emission peak are due to SiV centers in DNDs.

and silicon vacancy (SiV) centers.<sup>[4]</sup> For these properties, it is expected that fluorescent nanodiamonds can be useful for various applications, such as bioimaging,<sup>[5,6]</sup> quantum sensors,<sup>[7–10]</sup> and quantum information devices.<sup>[11–14]</sup>

Compared with nanodiamonds produced by milling large diamonds synthesized by chemical vapor deposition (CVD) and high-pressure high-temperature (HPHT) processes, detonation nanodiamonds (DNDs)<sup>[15]</sup> have smaller primary particle sizes (about 5 nm) and are more uniform in size and shape. They are also affordable through mass production by economical synthesis methods. Moreover, DNDs can exhibit fluorescence from color centers such as NV centers<sup>[16]</sup> as nitrogen impurities are incorporated during the detonation synthesis process. Fluorescence and optically detected magnetic resonance (ODMR) signals from an NV center in an

isolated single-digit DND (<10 nm), embedded in a polymer matrix, have been successfully observed.<sup>[17]</sup> Fluorescent nanodiamonds of 5 nm in size would be a huge step toward realizing bioimaging and targeting of single biomolecules in their natural environment. However, it is well-known that NV centers in smaller nanodiamonds are not only less bright (smaller number of NV centers), but also may blink or be bleached due to charge state instability.<sup>[18,19]</sup>

## 1. Introduction

Fluorescent nanodiamonds containing color centers have attracted considerable attention as single photon emitters in many fields from life sciences to quantum technologies. Nanodiamonds combine physical and chemical stabilities, high biocompatibility through surface modification,<sup>[1,2]</sup> and photostable fluorescence represented by nitrogen vacancy (NV) centers<sup>[3]</sup>

K. Shimazaki, H. Kawaguchi, H. Takashima, S. Takeuchi  
Department of Electronic Science and Engineering  
Kyoto University  
Kyotodaigakukatsura, Nishikyo-ku, Kyoto 615-8510, Japan  
E-mail: takeuchi@kuee.kyoto-u.ac.jp

 The ORCID identification number(s) for the author(s) of this article can be found under <https://doi.org/10.1002/pssa.202100144>.

© 2021 The Authors. *physica status solidi (a)* applications and materials science published by Wiley-VCH GmbH. This is an open access article under the terms of the Creative Commons Attribution-NonCommercial-NoDerivs License, which permits use and distribution in any medium, provided the original work is properly cited, the use is non-commercial and no modifications or adaptations are made.

DOI: 10.1002/pssa.202100144

T. F. Segawa  
Laboratory for Solid State Physics  
ETH Zurich  
8093 Zürich, Switzerland  
E-mail: segawat@ethz.ch

T. F. Segawa, F. T.-K. So, D. Terada, M. Shirakawa  
Department of Molecular Engineering  
Graduate School of Engineering  
Kyoto University  
Nishikyo-Ku, Kyoto 615-8510, Japan

S. Onoda, T. Ohshima  
Takasaki Advanced Radiation Research Institute  
National Institutes for Quantum and Radiological Science and Technology  
1233 Watanuki, Takasaki, Gunma 370-1292, Japan

In contrast to many pure and high-quality diamonds, DNDs carry an inherent potential for fluorescence from color centers, due to the variety of metal impurities (Na, Al, Si, Ti, Fe, Cu, and many others) that were incorporated during the detonation synthesis.<sup>[20]</sup> An interesting candidate for a color center is the negatively charged SiV center.<sup>[4]</sup> It has excellent properties such as stable and bright emission (737 nm) in the biological window,<sup>[21,22]</sup> a narrow emission peak (linewidth of about 5 nm) at room temperature,<sup>[23–25]</sup> and a high Debye–Waller factor (about 70%).<sup>[21,22]</sup> The atomic structure of the SiV point defect is a “split-vacancy,” where the silicon atom is placed between two adjacent vacancies (missing carbon atoms in the diamond lattice).<sup>[4]</sup> Blinking but stable emission from a single SiV center in an ultrasmall nanodiamond (1.6 nm), isolated from a meteorite, has been reported.<sup>[26]</sup> DNDs containing SiV centers would be of interest as an alternative fluorescent nanodiamond with high stability, sharp emission (in strong contrast to NV centers), and very small size below 10 nm, which are required for bioimaging to detect single molecules and single proteins.<sup>[27]</sup> All-optical thermometry<sup>[28]</sup> and cathodoluminescence<sup>[29]</sup> would be possible applications for SiV-incorporated DNDs. Such DNDs could also be useful for coupling with nanophotonic devices as photonic crystal cavities,<sup>[30,31]</sup> optical nanofibers,<sup>[32–36]</sup> and nanofiber Bragg cavities.<sup>[37–41]</sup> This is because the small size can prevent photon loss by scattering between the nanophotonic devices and the nanodiamonds.

A first demonstration of DNDs containing SiV centers was recently reported by adding a silicon-containing reagent for the detonation synthesis.<sup>[42]</sup> However, the linewidth of the observed emission peaks in this work (the smallest reported linewidth was 16.6 nm) were more than twice as broad as those of nanodiamonds synthesized by other methods such as CVD and HPHT.<sup>[43]</sup>

In this article, we report an alternative method to create SiV centers with a sharp emission peak in DNDs by an annealing treatment at high temperature and high vacuum. As a starting material, we used electron-irradiated DNDs. By annealing at up to 1100 °C in high vacuum,<sup>[44,45]</sup> SiV centers were created in the samples. A sharp emission line with the linewidth of 7.7 nm was observed at 737 nm, which is in good agreement with the emission line of SiV centers. This linewidth is comparable with that of the nanodiamonds created by CVD.<sup>[23]</sup> Furthermore, from the comparison with annealing at 800 °C, it was found that the high temperature annealing step at 1100 °C is needed for the formation of SiV centers in DNDs. The fluorescence lifetime of SiV centers in DNDs was determined to be  $0.4 \pm 0.04$  ns.

## 2. Sample Preparation and Characterization

As samples, we used colloidal solutions of DNDs (NanoAmando, NanoCarbon Research Institute). The size of the particles was estimated to be 5 nm by dynamic light scattering (DLS).<sup>[46]</sup> The concentration of Si impurities was estimated to be a few hundred ppm.<sup>[20]</sup> On average, this corresponds to a few silicon atoms per DND particle. The origin of silicon atoms could come from impurities in the reagents.<sup>[47]</sup> However, the nature of the silicon impurities is unknown. The DNDs were freeze dried

before electron irradiation. The irradiation fluence and energy were  $5 \times 10^{18} \text{ e}^- \text{ cm}^{-2}$  and 2 MeV, respectively. Electron irradiation of DND powder took place at room temperature. After irradiation, the DNDs were treated with the boiling acid method and finally washed with NaOH.<sup>[46]</sup>

Small amounts of DNDs dispersed in Milli-Q water were spin-coated onto silicon substrates. The silicon substrates were preannealed at 1200 °C under vacuum conditions (about  $10^{-5}$  Pa) to remove a thin surface layer of SiO<sub>2</sub>. When the samples were directly dispersed on the silicon substrates and annealed at 1100 °C, they disappeared from the substrate, possibly due to a reaction with the melted thin natural oxide film on the silicon. To increase the probability of finding SiV centers, we also prepared drop-casted samples, fabricated by directly dropping a small volume of DNDs dispersed in Milli-Q water onto the cleaned silicon substrates with a thermally oxidized layer.

We annealed the samples using an annealing process in high vacuum and at high temperature.<sup>[44,45]</sup> The annealing procedure consisted of four consecutive steps: 1) 8 h at 800 °C in vacuum ( $<10^{-4}$  Pa), 2) 1 h at 480 °C in air, 3) 2 h at 1100 °C in vacuum ( $<10^{-4}$  Pa), and 4) 1 h at 480 °C in air. Slow temperature ramps ( $<35$  °C per h) were used during the steps 2 and 4. The heating at less than 480 °C for about 1 h at ambient pressure to remove *sp*<sup>2</sup> carbon and contamination layers on the surface. This procedure is the same for DND powders and DNDs on substrates. To use an oil immersion objective lens with a high numerical aperture, the DNDs were transferred from the silicon substrate to a coverslip using an adhesive tape and heated to 480 °C for about 1 h in air to incinerate the tape.<sup>[48]</sup>

We analyzed the overall DND mass over the whole annealing procedure from steps 1) to 4). The annealing step reduced the mass of DNDs in powder from 12.5 to 9.2 mg, a reduction of about 25%. This includes oxidation of carbon in DNDs to CO<sub>2</sub>, but also loss of material to the walls of the annealing oven.

To analyze the structure of DNDs annealed at 1100 °C, we observed the samples using a transmission electron microscope (TEM; JEOL JEM-2200FS) with a resolution of 0.1 nm. **Figure 1a,b** shows two representative TEM images. The crystalline structures of diamond (e.g., white dotted circles) were clearly observed. The size of the diamond structure was less than 10 nm. A conversion of DNDs to onion-like carbon (OLC) was not observed. Therefore, we confirmed that DNDs survive our annealing process without structural modifications of the diamond core.

We further studied DND samples that were transferred from a silicon substrate to a coverslip by an atomic force microscope (AFM; FlexAFM, Nanosurf) equipped with a Si cantilever (OMCL-AC160TS, OLYMPUS). **Figure 1c** shows an AFM image of DNDs on a coverslip with a scan area of  $2 \times 2 \mu\text{m}^2$  at  $128 \times 128$  pixels. Many particles with different sizes are detected in the region of interest. The maximum height is about 260 nm. **Figure 1d** shows an AFM image of the square area including a small particle in **Figure 1c**. The size of the zoomed area is  $63 \times 63 \text{ nm}^2$  at  $32 \times 32$  pixels. The height and width of the particles are about 15 and 60 nm, respectively. This large size is likely to be due to aggregation of DNDs during the annealing process.<sup>[46]</sup>

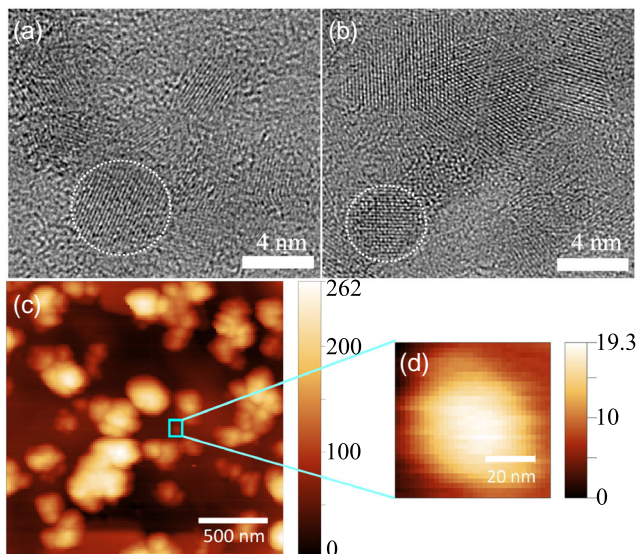


**Figure 1.** a,b) TEM images of electron-irradiated DNDs annealed at 1100 °C. c) AFM image of DNDs on coverslip. d) AFM image of the square area in (c).

### 3. Experimental Section

We evaluated the DNDs using a custom confocal microscope, shown in **Figure 2**. As a light source, we used a continuous-wave laser with a wavelength of 685 nm. The excitation power of the laser was about 3 mW in front of the objective. To prevent the tail of the laser light from overlapping with the fluorescence of the SiV centers, the light around 685 nm was selected by a bandpass filter and a short pass filter of 715 nm. The excitation laser reflected by a dichroic mirror was focused on the sample by an oil immersion objective lens with a numerical aperture of 1.4. The samples were scanned at steps of 200 nm using a 3D piezo stage. The fluorescence was collected by the same objective

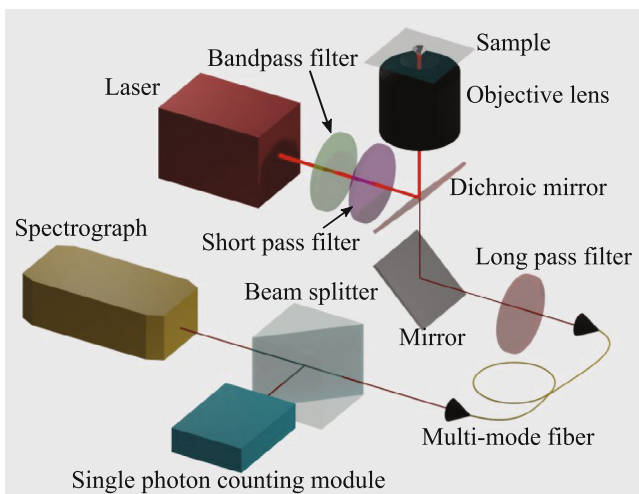


**Figure 2.** Experimental setup for confocal microscopy.

and coupled into a multimode fiber with a core diameter of about 10  $\mu\text{m}$  after being filtered by the dichroic mirror and a long pass filter of 715 nm. To measure confocal images, the fluorescence after passing through the multimode fiber was measured by a single photon counting module (SPCM; SPCM-AQR-12, PerkinElmer). Emission spectra were measured by an imaging spectrograph (Oriel, MS257) equipped with a charge coupled device (CCD) camera (Andor DU4200E). To measure the fluorescence lifetime of the emitters, we used a pulse laser with a pulse duration of about 40 ps at an excitation wavelength of 680 nm (PiL069X, Advanced laser diode systems). The output signal from the SPCM was analyzed by a time-correlated single photon counting module (SPC-130, Becker & Hickl) with the reference derived from the laser pulses. All the experiments were carried out at room temperature.

## 4. Experimental Results for Samples Annealed at 1100 °C

### 4.1. Confocal Images and Fluorescence Spectra of Spin-Coated DND Samples

We describe the experimental results for DNDs annealed at 1100 °C. To characterize the fluorescence from spin-coated DNDs, we took confocal microscope images, as shown in **Figure 3a**. The images show many bright spots with different intensities in the observed area. **Figure 3b** shows the emission spectra of the numbered bright spots in **Figure 3a** (A-1, A-2, A-3, A-4). Note that, light with wavelengths shorter than 722 nm is blocked by the long pass filter. A-1 (black line) shows a sharp emission peak at a wavelength of 738 nm, which corresponds to the zero-phonon line (ZPL) of an SiV center. The linewidth of A-1 is about 7.7 nm, which is comparable with the linewidth of HPHT nanodiamonds implanted Si ions at room temperature.<sup>[45]</sup> However, this sharp peak overlaps with a broad background emission peak, which is related to the emission from other defect centers. The shape of the spectrum of A-2 (red line) is similar to the broad background spectrum observed in A-1 without a SiV ZPL signature. Also for A-3 and A-4 (green and blue lines, respectively), there are no ZPLs from SiV centers.

To search for other DNDs showing the characteristic emission of SiV centers, we took a confocal image at a different area of the same sample [**Figure 3c**], and several further bright spots were observed in this area. **Figure 3d** shows the emission spectra of the bright spots in **Figure 3c** (A-5, A-6, A-7, A-8, A-9). A-5 (black line) shows a broad emission peak at 741 nm. The linewidth of A-5 is about 15 nm, which is considerably larger than that of A-1. At the same time, the intensity of A-5 is about 1 order of magnitude larger (above the background signal). We believe that the larger linewidth of A-5 is caused by inhomogeneous broadening from a multitude of SiV centers in various DNDs (with different strains, etc.) overlapping this confocal spot. A-6, A-7, A-8, and A-9 (red, green, blue, and light blue lines, respectively) show no emission peaks of SiV centers.

**Figure 3e** shows a confocal image of a third area of the same sample. Both A-10 and A-11 show sharp emission peaks (black

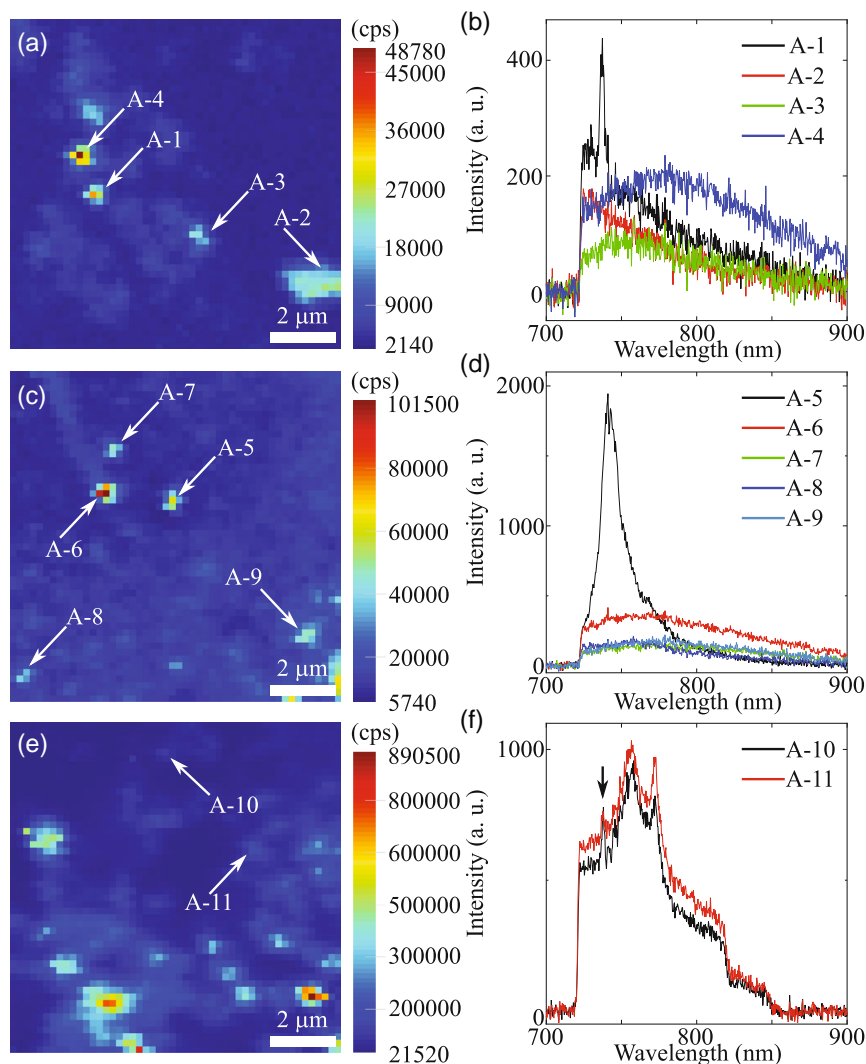


**Figure 3.** a,c,e) Confocal images and b,d,f) corresponding PL spectra of spin-coated DNDs after electron irradiation and annealing at 1100 °C. b,d,f) The images are the PL spectra of the bright spot in (a,c,e), respectively. The black arrow in (f) is the position of the emission line of SiV centers at 737 nm.

arrow) at 738 nm over three broad peaks. The overlap of these peaks could be due to the fact that DNDs containing SiV and other DNDs are agglomerated at the excitation spot.

Our study proves that Si atomic impurities as precursors for SiV centers are naturally present inside the diamond core of untreated DNDs. In this study, we discovered SiV centers in about 10% of bright spots of the spin-coated sample.

#### 4.2. Confocal Images and Fluorescence Spectra of Drop-Casted DND Samples

To further confirm the creation of SiV centers in DNDs, we measured the drop-casted samples, which have a higher density of DNDs than the spin-coated samples. Figure 4a shows a confocal scanning image. The inset of Figure 4a shows an optical microscope image around the scanning area taken by an electron-multiplying charge-coupled device (EMCCD) camera.

Particles with a size of about 1  $\mu\text{m}$ , due to aggregation, are observed. Figure 4b shows the emission spectrum of a bright spot (A-12). Light of wavelength less than 722 nm is blocked by a long pass filter and light of wavelength larger than 768 nm is blocked by a short pass filter. An asymmetric peak is observed at a wavelength of 736.4 nm. Note that, the origin of the broad peak with wavelengths larger than 740 nm is mainly background light emitted from the cover slip (see Figure 6b). The inset of Figure 4b shows the second-order correlation function of this bright spot. No dip is observed at zero delay, due to the formation of multiple SiV centers in the aggregation of DNDs and the presence of background light.

We measured another area of the same sample to further investigate the emission from SiV centers in drop-casted DND samples. Figure 4c shows the confocal scanning image. We measured the emission spectra of the bright spots (A-13, A-14, A-15, and A-16) observed in this scanning image, as

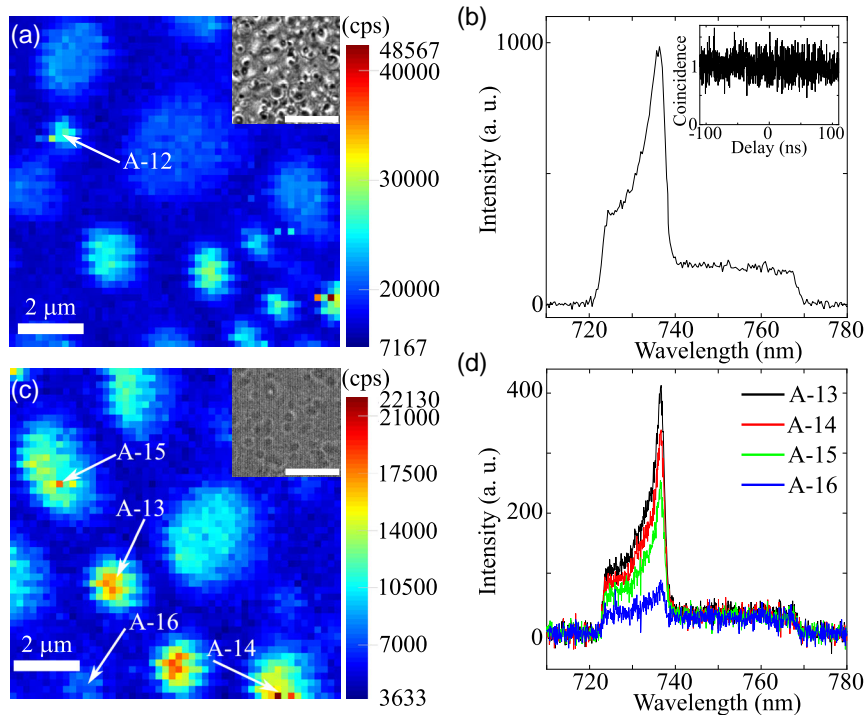


**Figure 4.** a,c) Scanning confocal images and b,d) emission spectra of drop-casted DNDs after electron irradiation and annealing at 1100 °C. The insets of (a,c) show optical microscope images taken by an EMCCD camera. The length of the scale bars is 10 μm. The inset of (b) shows the result of the second-order correlation function of A-12.

shown in Figure 4d. A sharp peak over a broad peak is observed at a wavelength of 736.4 nm for all the measured spots. The linewidths of the observed peaks are as narrow as those of nanodiamonds synthesized by CVD and followed by milling process.<sup>[43]</sup>

### 4.3. Fluorescence Lifetime Measurement

To support evidence of the emission from SiV centers, we measured the fluorescence lifetime of these emitters using the drop-casted DND sample. To reduce the effect of background

emission, we used a band pass filter (740 ± 13 nm). **Figure 5a** shows the emission spectrum and **Figure 5b** shows the corresponding decay curve. As shown in the inset of **Figure 5b**, the decay is exponential. The lifetime was estimated to be 0.4 ns. The average lifetime of 15 bright spots in confocal images was 0.4 ± 0.04 ns, which is within the reported range of the lifetime of SiV centers in 130 nm-sized nanodiamonds (0.2–2 ns).<sup>[21]</sup> This result supports that the emission peaks at around 738 nm are related to SiV centers in DNDs. Note that, it is assumed that this fast decay could be due to the nonradiative decay channel caused by local strain and degradation of crystal quality in DNDs.<sup>[21]</sup>

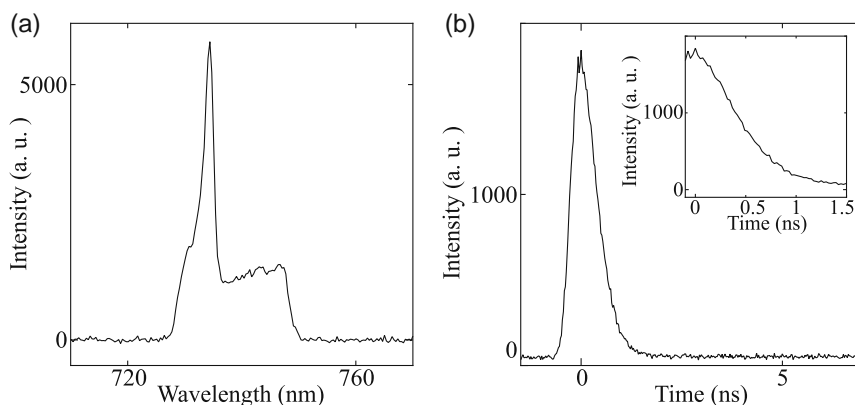


**Figure 5.** a) Emission spectrum and b) decay curve of the fluorescence of drop-casted DNDs after electron irradiation and annealing at 1100 °C. Note that, a band pass filter (740 ± 13 nm) was used to reduce the background emission. The inset of (b) is the magnified view of the decay curve from -0.1 to 1.5 ns.

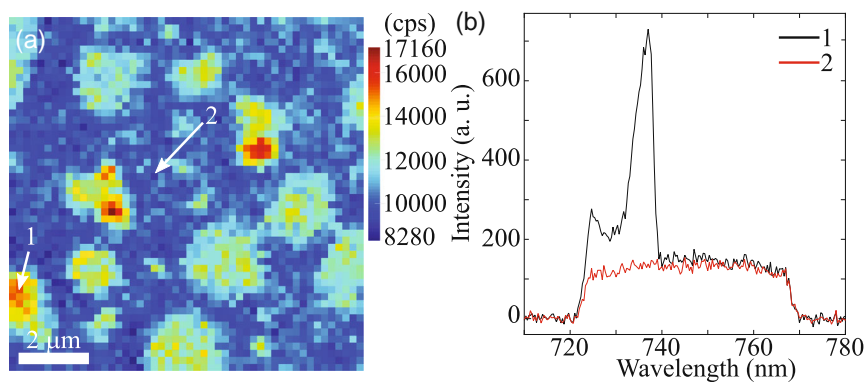


**Figure 6.** a) Scanning confocal image and b) emission spectra of drop-casted DNDs without electron irradiation after annealing at 1100 °C.

#### 4.4. Comparison between the Samples with and without Electron Irradiation

To clarify the reason of the asymmetric peak shapes of the spectra in Figure 4b,d, we measured the samples without electron irradiation, which had undergone the same high-temperature annealing treatment as drop-casted DND samples. As a representative example, the emission spectrum of a bright spot in Figure 6a is shown as a black line in Figure 6b. The shape of the peak observed at around 737 nm with a linewidth of 5.3 nm was clearly more symmetric than in the case of DND samples after electron irradiation. Note that, the remaining small asymmetry is due to the existence of SiV centers with different emission wavelengths, which are caused by the crystal strain. A red line in Figure 6b is the emission spectrum at the dark spot in Figure 6a. This spot shows only a broad emission peak, which is observed in the bright spots. This would be due to the background light from the cover slip. From this comparison with DNDs without electron irradiation, we considered that the asymmetric shape for DNDs with electron irradiation is related to the electron irradiation process. Electron irradiation can cause stress and damage in DNDs. These may cause the asymmetric shape of the peak.<sup>[21]</sup> In addition, electron irradiation in general creates other defect centers in diamond. If the emission from the defect

centers almost overlaps with the emission peak from SiV centers, it is likely that the emission peak is observed as a strong asymmetric shape. As two separated peaks in the emission spectrum of DNDs without electron irradiation can be identified (SiV ZPL and a peak at about 725 nm), we conclude that the asymmetric shapes in drop-casted DND samples after electron irradiation (Figure 4) stem from the overlap of the SiV center with the emission from another unassigned defect center.

#### 5. Experimental Results for Samples Annealed at 800 °C

To investigate the effect of annealing at 1100 °C, we measured electron-irradiated DND samples annealed at only 800 °C (only steps 1) and 2) in our annealing protocol) and compared them using the drop-casted samples, which have a higher density of DNDs than the spin-coated samples. Figure 7a shows a confocal scanning image of this sample. Many bright spots appear in the observed area. Figure 7b shows the emission spectra of the bright spots (B-1, B-2, and B-3). All the spots show emission spectra with three peaks with wavelengths of 725, 758, and 773 nm. These three peaks are not due to silicon in DND, but other impurities

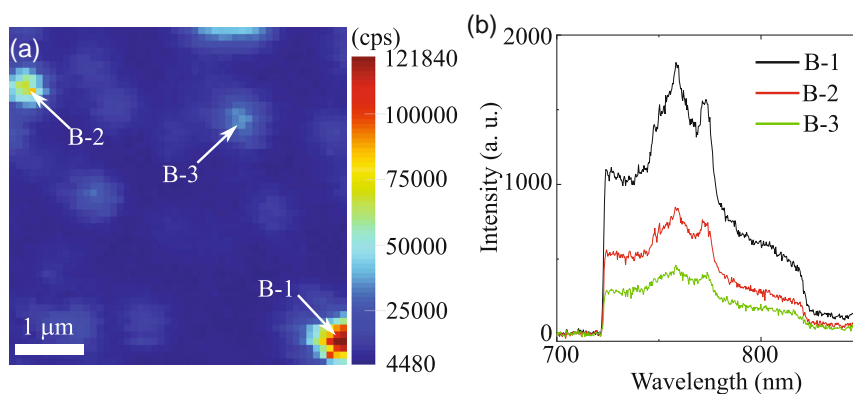


**Figure 7.** a) Scanning confocal image and b) emission spectra for of drop-casted DNDs after electron irradiation and annealing at 800 °C. No sharp emission lines from SiV centers at around 737 nm were observed.

such as nitrogen, as these peaks have been observed in commercial HPHT nanodiamonds without Si ion implantation (MSY 0–0.05, Microdiamant).<sup>[45]</sup> Similarly, we could not observe emission peaks of SiV centers in unannealed samples (not shown). Therefore, we conclude that high temperature annealing at 1100 °C is indispensable for the formation of SiV centers in DNDs.

## 6. Discussion

One key question is, if the structure of the 5 nm DNDs is affected by the annealing temperature of 1100 °C. It has been shown that annealing of DNDs in vacuum above 700 °C leads to gradual change in their structure and finally to carbon onions.<sup>[49]</sup> However, we could not find the structure of carbon onions in our TEM measurement. Therefore, we conclude that DNDs survive our high-temperature annealing condition without structural changes in the diamond lattice. It was recently reported that the formation of  $sp^2$  layer on the bulk diamond surface can be increased by shortening the ramp time and thus increasing the peak pressure during the vacuum anneal.<sup>[50]</sup> Therefore, we believe that our slow ramp rate (<35 °C per hour) could play an important role in avoiding the graphitization of DNDs to carbon onions.

Only the spectrum of A-5 in Figure 3 showed a typical emission spectrum of SiV centers, which reminds of SiV centers in bulk or larger nanodiamonds. As the peak intensity in the spectrum of A-5 was about ten times larger than the broad emission peak observed in the spectrum of A-1, it is considered that there were many more SiV centers in the spot of A-5. This led to a strong SiV photoluminescence (PL) signal with respect to the broad background emission peak, which had a comparable intensity in all spots. In solid-state materials, the linewidth of the emission peak increases with the number of emitters through inhomogeneous broadening. This explains the broader linewidth of the spectrum of spot A-5 with respect to the one of A-1.

In a recent study, SiV centers in nanodiamonds originating from CVD synthesis followed by milling were categorized in two groups.<sup>[23]</sup> A vertical (“V”) group with a narrow central wavelength distribution ( $\approx 730$ –742 nm), but rather large variation in linewidths (5–17 nm), compared with a horizontal (“H”) group, with a very broad central wavelength distribution ( $\approx 715$ –835 nm) but narrower linewidths (1–4 nm). Group “V” was assigned to the SiV center with the known structure, where strain in the diamond lattice leads to shifts of the central emission wavelengths. The identity of the defect behind the spectra of group “H,” possibly associated with silicon, however remains unknown.<sup>[23]</sup> Importantly, all the SiV signals observed in our samples can be assigned to group “V,” i.e., having the SiV center with the known structure of the split vacancy.

Interestingly, our findings on the formation of SiV centers in DNDs contrasts to those of NV centers in DNDs. DNDs contain a substantial concentration of NV centers without annealing or irradiation, and they form further NV centers through electron irradiation without the need for subsequent annealing.<sup>[46]</sup> This anomalous behavior is unique to DNDs. However, SiV centers seem to be formed in DNDs in a similar way than in larger nanodiamonds or bulk diamond: even a high-temperature annealing

step at 1100 °C appears to be a prerequisite for their formation. This might be related to the fact that SiV centers contain two vacancies where NV centers include only one. The advantage of a first annealing step at 800 °C could be related to the divacancy, which is mobile in the range of  $\approx 600$ –850 °C.<sup>[51–53]</sup> At higher temperatures, vacancy chains are formed. In the second annealing step, silicon defects could move into these divacancies. The effect of electron irradiation on SiV formation in DNDs is still unclear and will be further investigated by studying isolated DNDs, where a quantitative analysis is possible.

## 7. Conclusion and Future Prospects

In conclusion, we have demonstrated characteristic fluorescence from SiV centers in DNDs. To form SiV centers, the DNDs were annealed at 1100 °C in high vacuum. The starting material used were standard DNDs, i.e., not made of silicon-containing detonation reagents and without additional Si ion implantation. Therefore, we believe that SiV centers originated from Si defects in the DND crystal lattice, which were formed during the detonation synthesis. From the TEM measurement, we found that the DND structure was unaffected during the annealing process at 1100 °C in high vacuum. When DNDs transferred to a microscope cover slip were excited with a laser of 685 nm, a sharp emission peak at 737 nm with a linewidth of 7.7 nm was observed, which is consistent with the emission line of SiV centers. This narrow linewidth could be a benefit to room-temperature sensing applications such as all-optical thermometry or cathodoluminescence. The lifetime of SiV centers in DNDs was determined to be  $0.4 \pm 0.04$  ns.

In a next step, we plan to study the deaggregation of SiV-containing DNDs using bead-assisted sonic disintegration (BASD).<sup>[24,54]</sup> This will allow us to produce large quantities of deaggregated colloidal solutions of SiV-DNDs. Evaluating such DNDs using a confocal microscope combined with an AFM will enable the study of fluorescent and photonic properties of SiV centers in individual, isolated DNDs. These experiments will facilitate the estimation of the density of SiV centers in DNDs. Such DNDs would be useful as photo-stable fluorescent nanodiamonds with small sizes of less than 10 nm with applications in bioimaging or quantum information technologies using nanophotonic devices.

## Acknowledgements

K.S., H.K. and H.T. contributed equally to this work. The authors gratefully acknowledge financial support in the form of Kakenhi Grants-in-Aid (nos. 21H04444, 26220712, 20H00453, 18K19297, and 19K03686) from the Japan Society for the Promotion of Science (JSPS), the CREST program of the Japan Science and Technology Agency (JST) (JPMJCR1674), and the MEXT Quantum Leap Flagship Program (MEXT Q-LEAP) (JPMXS0118067634). H. T. acknowledges the support of the Matsuo Foundation. T.F.S. acknowledges The Branco Weiss Fellowship—Society in Science, administered by the ETH Zurich, and Prof. Shirakawa for hosting him as a Guest Research Associate at Kyoto University. The authors thank Prof. Kei Kobayashi at Kyoto University for helpful advice on AFM measurements, Prof. Mitsuru Funato and Prof. Ryota Ishii for helpful advice on substrates, and Dr. Eiji Osawa, NanoCarbon Research Institute (Ueda, Japan), for kindly providing detonation-synthesized nanodiamonds. A part of this work was supported by

Kyoto University Nano Technology Hub as a program of "Nanotechnology Platform" of the Ministry of Education, Culture, Sports, Science and Technology (MEXT), Japan, grant no. JPMXP09A21KT0008.

Open access funding provided by Eidgenössische Technische Hochschule Zurich.

[Correction added on April 7, 2022, after first online publication: CSAL funding statement has been added.]

## Conflict of Interest

The authors declare no conflict of interest.

## Data Availability Statement

The data that support the findings of this study are available from the corresponding author upon reasonable request.

## Keywords

detonation nanodiamonds, nanodiamonds, narrow emission lines, silicon-vacancy centers

Received: March 17, 2021

Revised: June 28, 2021

Published online: July 29, 2021

- [1] S.-J. Yu, M.-W. Kang, H.-C. Chang, K.-M. Chen, Y.-C. Yu, *J. Am. Chem. Soc.* **2005**, *127*, 17604.
- [2] V. N. Mochalin, O. Shenderova, D. Ho, Y. Gogotsi, *Nat. Nanotechnol.* **2012**, *7*, 11.
- [3] I. Aharonovich, A. D. Greentree, S. Praver, *Nat. Photonics* **2011**, *5*, 397.
- [4] C. Bradac, W. Gao, J. Forneris, M. E. Trusheim, I. Aharonovich, *Nat. Commun.* **2019**, *10*, 5625.
- [5] Y. Y. Hui, C.-L. Cheng, H.-C. Chang, *J. Phys. D Appl. Phys.* **2010**, *43*, 374021.
- [6] M. D. Torelli, N. A. Nunn, O. A. Shenderova, *Small* **2019**, *15*, 1902151.
- [7] L. P. McGuinness, Y. Yan, A. Stacey, D. A. Simpson, L. T. Hall, D. Maclaurin, S. Praver, P. Mulvaney, J. Wrachtrup, F. Caruso, R. E. Scholten, L. C. L. Hollenberg, *Nat. Nanotechnol.* **2011**, *6*, 358.
- [8] G. Kucsko, P. C. Maurer, N. Y. Yao, M. Kubo, H. J. Noh, P. K. Lo, H. Park, M. D. Lukin, *Nature* **2013**, *500*, 54.
- [9] T. Rendler, J. Neburkova, O. Zemek, J. Kotek, A. Zappe, Z. Chu, P. Cigler, J. Wrachtrup, *Nat. Commun.* **2017**, *8*, 14701.
- [10] T. Fujisaku, R. Tanabe, S. Onoda, R. Kubota, T. F. Segawa, F. T.-K. So, T. Ohshima, I. Hamachi, M. Shirakawa, R. Igarashi, *ACS Nano* **2019**, *13*, 11726.
- [11] M. Pelton, *Nat. Photonics* **2015**, *9*, 427.
- [12] M. Pelton, C. Santori, J. Vučković, B. Zhang, G. S. Solomon, J. Plant, Y. Yamamoto, *Phys. Rev. Lett.* **2002**, *89*, 233602.
- [13] Q. A. Turchette, C. J. Hood, W. Lange, H. Mabuchi, H. J. Kimble, *Phys. Rev. Lett.* **1995**, *75*, 4710.
- [14] H. P. Specht, C. Nölleke, A. Reiserer, M. Uphoff, E. Figueroa, S. Ritter, G. Rempe, *Nature* **2011**, *473*, 190.
- [15] E. Ōsawa, *Diamond Relat. Mater.* **2007**, *16*, 2018.
- [16] B. R. Smith, D. W. Inglis, B. Sandnes, J. R. Rabeau, A. V. Zvyagin, D. Gruber, C. J. Noble, R. Vogel, E. Ōsawa, T. Plakhotnik, *Small* **2009**, *5*, 1649.
- [17] C. Bradac, T. Gaebel, N. Naidoo, M. J. Sellars, J. Twamley, L. J. Brown, A. S. Barnard, T. Plakhotnik, A. V. Zvyagin, J. R. Rabeau, *Nat. Nanotechnol.* **2010**, *5*, 345.
- [18] C. Bradac, T. Gaebel, N. Naidoo, J. R. Rabeau, A. S. Barnard, *Nano Lett.* **2009**, *9*, 3555.
- [19] C. Bradac, T. Gaebel, C. I. Pakes, J. M. Say, A. V. Zvyagin, J. R. Rabeau, *Small* **2013**, *9*, 132.
- [20] P. N. Nesterenko, D. Mitev, B. Paull, in *Nanodiamonds*, (Ed: J.-C. Arnault), Elsevier, Amsterdam **2017**, pp. 109–130.
- [21] E. Neu, D. Steinmetz, J. Riedrich-Möller, S. Gsell, M. Fischer, M. Schreck, C. Becher, *New J. Phys.* **2011**, *13*, 025012.
- [22] A. Sipahigil, K. D. Jahnke, L. J. Rogers, T. Teraji, J. Isoya, A. S. Zibrov, F. Jelezko, M. D. Lukin, *Phys. Rev. Lett.* **2014**, *113*, 113602.
- [23] S. Lindner, A. Bommer, A. Muzha, A. Krueger, L. Gines, S. Mandal, O. Williams, E. Londero, A. Gali, C. Becher, *New J. Phys.* **2018**, *20*, 115002.
- [24] E. Neu, C. Arend, E. Gross, F. Guldner, C. Hepp, D. Steinmetz, E. Zscherpel, S. Ghodbane, H. Sternschulte, D. Steinmüller-Nethl, Y. Liang, A. Krueger, C. Becher, *Appl. Phys. Lett.* **2011**, *98*, 243107.
- [25] C. Chen, Y. Mei, J. Cui, X. Li, M. Jiang, S. Lu, X. Hu, *Carbon* **2018**, *139*, 982.
- [26] I. I. Vlasov, A. A. Shiryaev, T. Rendler, S. Steinert, S.-Y. Lee, D. Antonov, M. Vörös, F. Jelezko, A. V. Fisenko, L. F. Semjonova, J. Biskupek, U. Kaiser, O. I. Lebedev, I. Sildos, P. R. Hemmer, V. I. Konov, A. Gali, J. Wrachtrup, *Nat. Nanotechnol.* **2014**, *9*, 54.
- [27] M. H. Alkahtani, F. Alghannam, L. Jiang, A. Almethen, A. A. Rampersaud, R. Brick, C. L. Gomes, M. O. Scully, P. R. Hemmer, *Nanophotonics* **2018**, *7*, 1423.
- [28] C. T. Nguyen, R. E. Evans, A. Sipahigil, M. K. Bhaskar, D. D. Sukachev, V. N. Agafonov, V. A. Davydov, L. F. Kulikova, F. Jelezko, M. D. Lukin, *Appl. Phys. Lett.* **2018**, *112*, 203102.
- [29] H. Zhang, I. Aharonovich, D. R. Glenn, R. Schalek, A. P. Magyar, J. W. Lichtman, E. L. Hu, R. L. Walsworth, *Small* **2014**, *10*, 1908.
- [30] J. Wolters, A. W. Schell, G. Kewes, N. Nüsse, M. Schoengen, H. Döscher, T. Hannappel, B. Löchel, M. Barth, O. Benson, *Appl. Phys. Lett.* **2010**, *97*, 141108.
- [31] B.-S. Song, S. Noda, T. Asano, Y. Akahane, *Nat. Mater.* **2005**, *4*, 207.
- [32] M. Fujiwara, K. Toubaru, T. Noda, H.-Q. Zhao, S. Takeuchi, *Nano Lett.* **2011**, *11*, 4362.
- [33] R. Yalla, F. Le Kien, M. Morinaga, K. Hakuta, *Phys. Rev. Lett.* **2012**, *109*, 063602.
- [34] T. Schröder, M. Fujiwara, T. Noda, H.-Q. Zhao, O. Benson, S. Takeuchi, *Opt. Express* **2012**, *20*, 10490.
- [35] M. Fujiwara, K. Yoshida, T. Noda, H. Takashima, A. W. Schell, N. Mizuochi, S. Takeuchi, *Nanotechnology* **2016**, *27*, 455202.
- [36] A. W. Schell, H. Takashima, T. T. Tran, I. Aharonovich, S. Takeuchi, *ACS Photonics* **2017**, *4*, 761.
- [37] A. W. Schell, H. Takashima, S. Kamioka, Y. Oe, M. Fujiwara, O. Benson, S. Takeuchi, *Sci. Rep.* **2015**, *5*, 9619.
- [38] H. Takashima, M. Fujiwara, A. W. Schell, S. Takeuchi, *Opt. Express* **2016**, *24*, 15050.
- [39] W. Li, J. Du, S. N. Chormaic, *Opt. Lett.* **2018**, *43*, 1674.
- [40] H. Takashima, A. Fukuda, H. Maruya, T. Tashima, A. W. Schell, S. Takeuchi, *Opt. Express* **2019**, *27*, 6792.
- [41] P. Romagnoli, M. Maeda, J. M. Ward, V. G. Truong, S. N. Chormaic, *Appl. Phys. B* **2020**, *126*, 111.
- [42] Y. Makino, T. Mahiko, M. Liu, A. Tsurui, T. Yoshikawa, S. Nagamachi, S. Tanaka, K. Hokamoto, M. Ashida, M. Fujiwara, N. Mizuochi, M. Nishikawa, *Diamond Relat. Mater.* **2021**, *112*, 108248.
- [43] J. N. Becker, B. Pingault, D. Groß, M. Gündoğan, N. Kukharchyk, M. Markham, A. Edmonds, M. Atatüre, P. Bushev, C. Becher, *Phys. Rev. Lett.* **2018**, *120*, 053603.
- [44] R. E. Evans, A. Sipahigil, D. D. Sukachev, A. S. Zibrov, M. D. Lukin, *Phys. Rev. Appl.* **2016**, *5*, 044010.

- [45] H. Takashima, A. Fukuda, K. Shimazaki, Y. Iwabata, H. Kawaguchi, A. W. Schell, T. Tashima, H. Abe, S. Onoda, T. Ohshima, S. Takeuchi, *Opt. Mater. Express* **2021**, *11*, 1978.
- [46] D. Terada, T. F. Segawa, A. I. Shames, S. Onoda, T. Ohshima, E. Ōsawa, R. Igarashi, M. Shirakawa, *ACS Nano* **2019**, *13*, 6461.
- [47] D. P. Mitev, A. T. Townsend, B. Paull, P. N. Nesterenko, *Carbon* **2013**, *60*, 326.
- [48] H. Takashima, H. Maruya, K. Ishihara, T. Tashima, K. Shimazaki, A. W. Schell, T. T. Tran, I. Aharonovich, S. Takeuchi, *ACS Photonics* **2020**, *7*, 2056.
- [49] M. Zeiger, N. Jäckel, V. N. Mochalin, V. Presser, *J. Mater. Chem. A* **2016**, *4*, 3172.
- [50] S. Sangtawesin, B. L. Dwyer, S. Srinivasan, J. J. Allred, L. V. Rodgers, K. De Greve, A. Stacey, N. Dontschuk, K. M. O'Donnell, D. Hu, D. A. Evans, C. Jaye, D. A. Fischer, M. L. Markham, D. J. Twitchen, H. Park, M. D. Lukin, N. P. De Leon, *Phys. Rev. X* **2019**, *9*, 031052.
- [51] J. N. Lomer, A. M. A. Wild, *Radiat. Eff.* **1973**, *17*, 37.
- [52] K. Iakoubovskii, A. Stesmans, *Phys. Rev. B* **2002**, *66*, 045406.
- [53] T. Yamamoto, T. Umeda, K. Watanabe, S. Onoda, M. L. Markham, D. J. Twitchen, B. Naydenov, L. P. McGuinness, T. Teraji, S. Koizumi, F. Dolde, H. Fedder, J. Honert, J. Wrachtrup, T. Ohshima, F. Jelezko, J. Isoya, *Phys. Rev. B* **2013**, *88*, 075206.
- [54] M. Ozawa, M. Inaguma, M. Takahashi, F. Kataoka, A. Krüger, E. Ōsawa, *Adv. Mater.* **2007**, *19*, 1201.